Open Access

Single-Mode Vertical-Cavity Surface-Emitting Laser Array With High Power and Narrow Far-Field Divergence Angle

Jin-Wei Shi, Senior Member, IEEE
Kai-Lun Chi
Jin-Hao Chang
Zhi-Rui Wei
Jia-Wei Jiang
Ying-Jay Yang
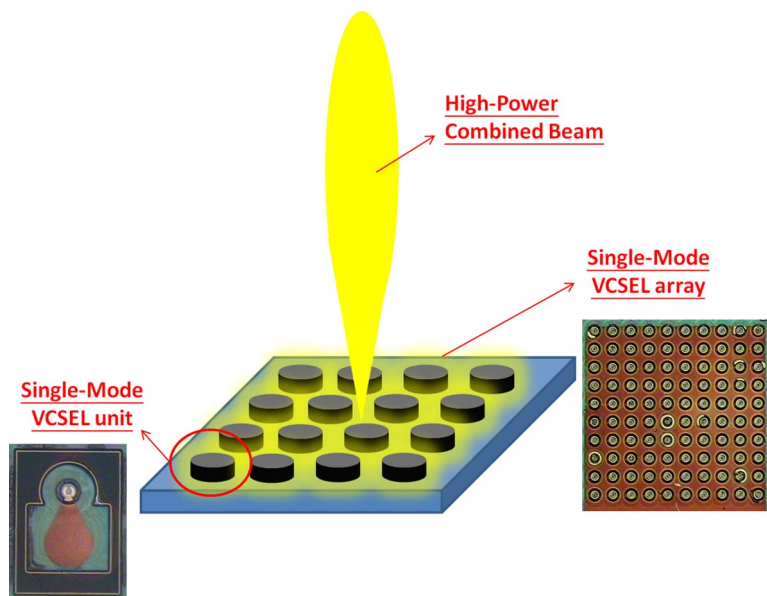
Single-Mode Vertical-Cavity Surface-Emitting Laser Array With High Power and Narrow Far-Field Divergence Angle

Jin-Wei Shi,[1] *Senior Member, IEEE*, **Kai-Lun Chi,**[1] **Jin-Hao Chang,**[1] **Zhi-Rui Wei,**[1] **Jia-Wei Jiang,**[1] **and Ying-Jay Yang**[2]

[1]Department of Electrical Engineering, National Central University, Taoyuan 320, Taiwan
[2]Department of Electrical Engineering, National Taiwan University, Taipei 106, Taiwan

Abstract: We demonstrate novel structures of an 850-nm vertical-cavity surface-emitting laser (VCSEL) array for high output power, single-lobe far-field pattern, and narrow divergence angle. By using the Zn-diffusion process with proper sizes of oxide-current-confined and Zn-diffusion apertures, each unit of VCSEL in the demonstrated array is highly single-mode (side-mode suppression ratio > 30 dB) with a narrow far-field divergence angle $(9°-10°)$ and high maximum single-mode output power ($\sim$6.3 mW). Due to the high uniformity of single-mode performance of each VCSEL unit, the 6×6 array exhibits an excellent lasing phenomenon, which includes single-lobe far-field pattern, weak in-phase coupling, narrowing of divergence angle (from 9° to 4°), and output power as high as around 104 mW. Furthermore, by measuring the bias-dependent output optical spectra in different positions of our array, the high similarity of these spectra indicates the excellent uniformity of our fabrication process for single-mode VCSEL.

Index Terms: Semiconductor lasers, laser beam combing.

1. Introduction

Vertical-cavity surface-emitting lasers (VCSELs) [1] have attracted much attention due to their several unique advantages, such as two-dimensional (2-D) array formation [2], [3], inexpensive device fabrication, and on-wafer characterization. High-output-power, high modulation speed, and a single-lobe (spot) output with a low divergence angle and circular symmetry far-field pattern of VCSEL are much desired for several applications, such as (free space) optical interconnects [4]–[6], laser printing, laser mouse [7], airborne light detecting and ranging (LIDAR) systems [8], and infrared lighting [9]. Increasing the effective diameter of the circular light-emitting aperture of a VCSEL is necessary to achieve a high output power. Extremely high output power (up to several watts level) by paralleling a few hundred to a few 10 000s multi-mode VCSELs with advanced thermal package has been successfully demonstrated [9]. However, due to the multi-mode characteristic of each VCSEL unit, the divergence angle of combined far-field pattern is as wide as $\sim$20°. In addition, the peak of combined 2-D far-field pattern is usually very spotty instead of a Gaussian like smooth profile [9]. Several methods have been developed for VCSELs with single-mode and single-lobe output, such
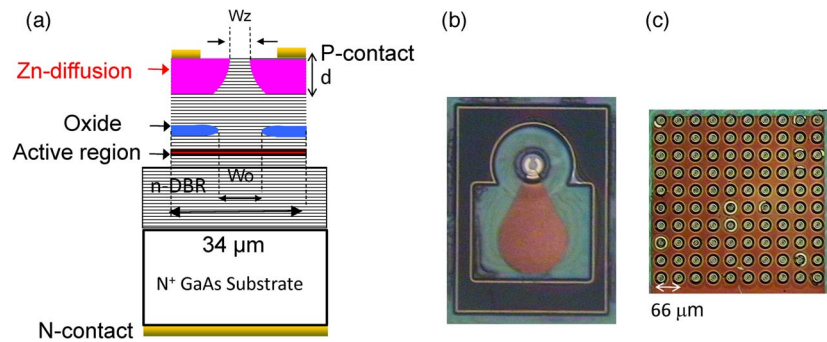
Fig. 1. (a) Conceptual cross-sectional view of unit VCSEL ($W_z/W_o/d$: 5/8/1.5 μm), (b) top-view of unit VCSEL, and (c) top-view of demonstrated 10 × 10 VCSEL array

as the surface relief structure [10], Zn-diffusion structure [11], the 2-D holey structure (photonic crystal) [12], [13], anti-resonant reflecting optical waveguide structure [14], [15], and the combined application of implant and oxide apertures [16]. However, the maximum single-mode output power of these reported VCSELs is usually less than 7 mW with a divergence angle at around 10° [10]–[16]. Recently, by combing the Zn-diffusion optical aperture and strained active layers [17]–[19], a (near) single-mode 850 nm VCSEL with excellent output power performance (~9 mW) has been demonstrated [20]. Furthermore, by using the photonic crystal (PC) based surface-emitting laser (array) structures, large area coherent lasing has been realized in order to further improve the performance in terms of power, beam shape, and divergence angle [21] of a single VCSEL. Such laser (array) can achieve excellent single-mode output power (~100 mW) under continuous wave (CW) operation with extremely narrow divergence angle (~2°) of circular symmetry far-field pattern [21]. Nevertheless, mass production of such device with complex 3-D nano-scale PC structure inside is really a challenge. In this paper, by using Zn-diffusion technique for optical mode control, we demonstrate a novel 2-D single-mode VCSEL array structure with excellent lasing performance. A stable (invariable) single-lobe/circular far-field pattern with narrow full-width half maximum (FWHM) divergence angle (4°–7°) under the full range of bias current and a high maximum single-lobe output power (104 mW) under CW operation can be achieved. Such excellent performance of proposed device structure indicates the high uniformity in our single-mode performance and weak in-phase (coherent) coupling between each VCSEL unit.

2. Device Structure and Fabrication

Fig. 1(a) and (b) shows the conceptual cross-sectional and top views of the demonstrated unit VCSEL, respectively. As shown in Fig. 1(a), there are three key parameters: W_Z, W_O, and d, which determine the mode characteristics of the device. Here, W_Z and W_O represent the diameter of Zn-diffusion aperture and oxide-confined aperture, respectively. d is the Zn-diffusion depth. In order to attain stable single-mode performance under the whole range of bias current of each unit VCSEL, the relative sizes of these three parameters must be carefully optimized [11]. First, the sizes of W_z and d must be usually less than 5 μm and deeper than 1 μm, respectively [11], [22]. This empirical criterion is valid due to the fact that we need a significant Zn-diffusion induced loss in the peripheral region of a small optical aperture (with a 5 μm diameter) to suppress the higher order mode. Second, we must let $W_O > W_Z$ in our single-mode structure to ensure that there is a significant Zn-diffusion induced internal loss (α_i) in our current-confined (gain) region. According to our measurement results, such condition is the key to ensure the high uniformity in single-mode lasing performance of each unit VCSEL of array [22]. Here, we chose the values of W_o, W_z, and d as 8, 5, and 1.5 μm, respectively. As shown in Fig. 1(a), the fabricated device has a ~34 μm diameter active mesa, and the n-type contact is realized on the bottom side of n-type GaAs substrate in order to uniform the current distribution especially in the array structure. The epitaxy-layer is the standard 850 nm VCSEL epi-layer structure (IEGENS-7-20) purchased from IQE, and the detail device fabrication processes
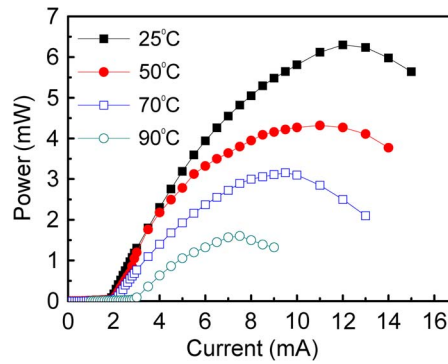
Fig. 2. The measured L-I curves under different ambient temperatures of unit VCSEL.

and epi-layer structure can be referred to our previous work [6], [11], [22]. Fig. 1(c) shows the top-view of fabricated 10 × 10 array. As can be seen, we simply parallel each unit VCSEL by connecting their p-type metals with a large metal pad for probing or wire bonding. All the unit devices are common ground through the use of bottom n-type contact layer on the n-type GaAs substrate. As specified in Fig. 1(c), the spacing between each unit VCSEL is 66 μm.

In contrast to most of the reported semiconductor laser arrays [2], [3], where each light-emission aperture shares the same optical cavity and its optical near-field usually has strong overlap (coupling), in our proposed array structure, the optical near field of each single-mode unit (aperture) is isolated by different mesa with a significant spacing (66 μm). The strong phase locking (coherent lasing) between different emitters and significant narrowing of the array's far-field divergence angle thus cannot be expected in our structure. Nevertheless, if each unit in our proposed array structure has very similar single-mode performance, we still can expect that the divergence angle of the array can be as narrow as that of a single-mode unit VCSEL and the total output power can be as high as the summation of power from all the VCSEL units.

3. Measurement Results

Fig. 2 shows the measured light output versus current (L-I) characteristics of a single VCSEL under different ambient temperatures. As can be seen, under room temperature (RT; 25 °C) operation, the single device exhibits a threshold current at 2 mA with a maximum single-mode power up to 6.3 mW. Such value is close to the record (~7 mW) of maximum single-mode output power of 850 nm VCSELs [10]–[12]. When the ambient temperature increases, our single device suffers from the problem of increasing in threshold current and degradation in differential quantum efficiency. Such phenomenon is very common and usually observed in the VCSELs. Although the static performance of our single laser degrades under high-temperature operation, it can still sustain single-mode characteristic. Fig. 3(a) and (b) shows the measured optical spectra and 2-D far-field pattern of the single device under different high bias currents (8–10 mA) at RT and 90 °C, respectively. We can clearly see that the excellent single-mode performance is still sustained even under high-temperature (90 °C) and high bias current operations (10 mA). Fig. 4 shows the measured L-I curves of 6 × 6 and 10 × 10 array, and the maximum output power (104 and 145 mW) for such two cases are also specified. Compared with the 6 × 6 array, the 10 × 10 array exhibits lower differential quantum efficiency and a lower averaged output saturation power from each unit single device (2.9 vs. 1.45 mW). This can be attributed to the higher required driving current (~2.3 times higher for the same output power) and more serious device heating in the 10 × 10 array structure. According to the measured saturation output power per unit device and the temperature dependent L-I curves, as shown in Fig. 2, the estimated junction temperature of 6 × 6 and 10 × 10 arrays is at around 70 and 90 °C, respectively.

Figs. 5–7 show the measured 1-D and 2-D far-field patterns of the single device, 6 × 6 array, and 10 × 10 array, respectively. Take the 6 × 6 array structure for example, if a perfectly (100%)
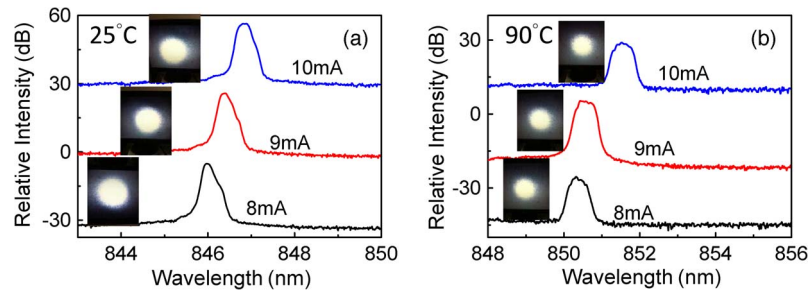
Fig. 3. The measured output optical spectra of unit VCSEL under different bias currents at room temperature (a) and 90 °C (b).
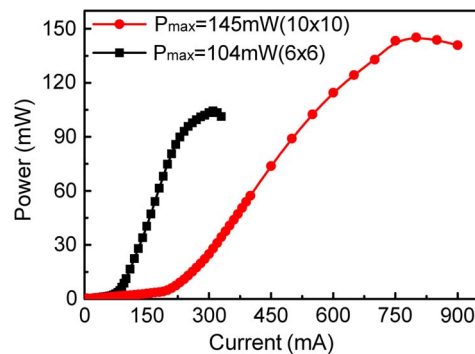

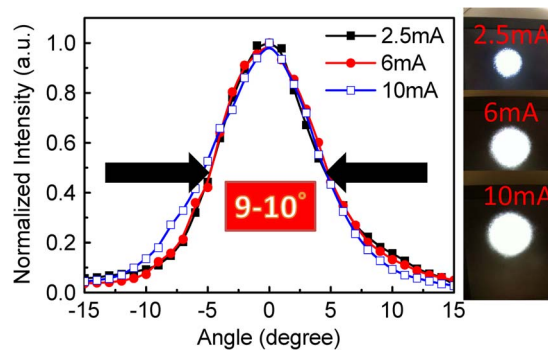Fig. 4. The measured L-I curves of 6 × 6 and 10 × 10 array.

Fig. 5. The measured 1-D and 2-D far-field patterns under different bias currents of unit VCSEL. The FWHM of divergence angle is specified.

phase-locking phenomenon happens in this structure with such a large area ($330 \times 330~\mu m^2$), the theoretical diffraction-limited divergence angle should be as small as 0.15°. As shown in Fig. 6, the measured far-field angle of (6 × 6) array is only slightly narrower ($\sim 4°$ vs. $\sim 9°$) than that of the single reference device. We can thus conclude that the observed phase-locking effect in our array is weak [23]. Such weak phase-locking phenomenon may be attributed to the overlapping (coupling) and feedback [24] of optical far-field from each single-mode unit, which has a long coherent length (time). In our case, the optical feedback might be originated from the unavoidable optical reflection from test setup. During our far-field measurement, if the relative distances between different optical components in our setup are changed, a slight variation in the measured values of divergence angle,
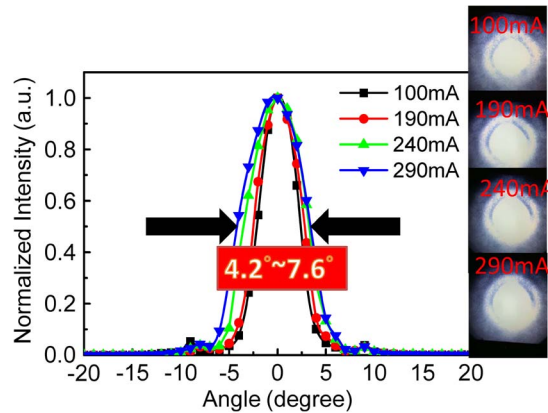
Fig. 6. The measured 1-D and 2-D far-field patterns under different bias currents of 6 × 6 array. The FWHM of divergence angle is specified.
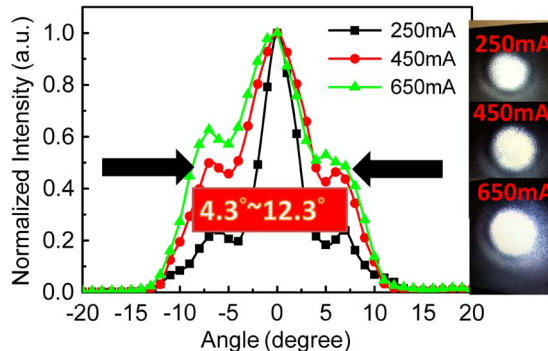

Fig. 7. The measured 1-D and 2-D far-field patterns under different bias currents of 10 × 10 array. The FWHM of divergence angle is specified.

which usually varies from 4° to 6°, would be observed. This result implies that we may further improve the far-field pattern of our proposed array by using the technique of device package to manipulate such feedback effect. In the multi-mode VCSEL array [9], such phenomenon rarely happens due to the fact that the coherent length (time) of each multi-mode beam is much shorter than that of single-mode beam, which should diminish the phase-locking (coherent) effect. With regard to the 10 × 10 array, as shown in Fig. 7, its measured 1-D and 2-D far-field patterns show two significant side-lobes when the bias current reaches ∼500 mA. The observed side-lobe is so called Newton's rings effect; the nulls and peaks in the measured far-field patterns correspond to constructive and deconstructive interference patterns of different single-mode output beams from each VCSEL unit, respectively. On the other hand, as shown in Fig. 6, for the case of our 6 × 6 array, such effect is not significant at all. This result can be possibly attributed to the fact that there are more VCSEL units in the 10 × 10 array out-of-phase single-mode lasing as compared to that in our 6 × 6 array, which would result in more significant interference pattern and broadening of far-field pattern. According to the above-mentioned measurement results, we can clearly see that our 6 × 6 array exhibits not only a smaller divergence angle (∼4° vs. ∼9°) of far-field pattern but also with a much higher maximum output power (104 vs. 6.3 mW) compared with those of single unit VCSEL. Furthermore, its single-spot and narrow far-field distribution can be sustained from near threshold until saturation. Such excellent result indicates that the single-mode performance of each unit VCSEL is very uniform.

Fig. 8 shows the measured 1-D far-field patterns of the single device, 6 × 6 array, and 10 × 10 array, at 6, 240, and 450 mA bias currents, respectively. We can clearly see that, compared with the
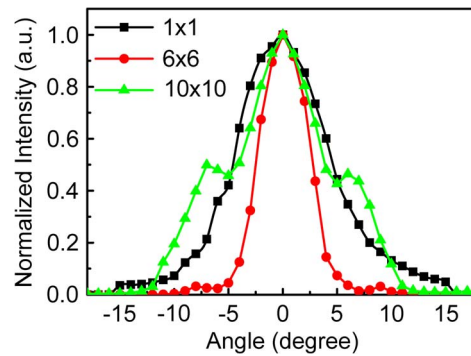
Fig. 8. The measured 1-D far-field patterns of single device, 6 × 6, and 10 × 10 array at 6, 190, and 450 mA bias currents, respectively.
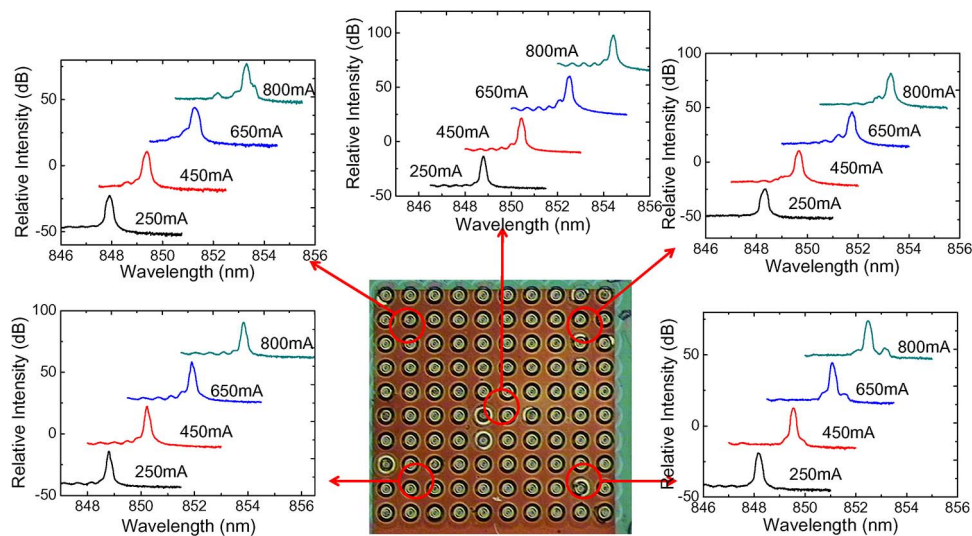

Fig. 9. The measured bias dependent output optical spectra in different portions of 10 × 10 array.

single device and 10 × 10 array, the 6 × 6 array has a narrower far-field angle, which indicates a larger number of in-phase coherent lasing elements in the array [23]. Fig. 9 shows the measured bias dependent output optical spectra of 10 × 10 array at different portions of the array. As can be seen, although the phase-locking between each unit VCSEL in the array is very weak as discussed, the measured spectra in different portions of the array are very similar, which indicates that the uniformity of single-mode performance of each VCSEL unit in our array is high.

Table 1 shows the benchmark of high-performance single-mode surface-emitting laser (SEL) array at 850 [13], [15] and 960 nm [25] wavelengths. We can clearly see that our demonstrated structure can achieve excellent slope efficiency with very-high output optical power and sustain a narrow far-field divergence angle among the reported single-mode SEL array structures [13], [15], [25].

4. Conclusion

In conclusion, we demonstrate a novel weak-coupling single-mode VCSEL array structure. By properly controlling the sizes of Zn-diffusion and oxide apertures, each unit VCSEL in the whole

TABLE 1

Comparison of figure of merit for state-of-art single-mode SEL array

	Kyoto University[25]	UWM[15]	UIUC[13]	This work (6x6)
Slope Efficiency(W/A)	0.4	0.045	0.3	0.6
Divergence Angle	< 2°	1.61°	3°	4.2~7.6°
Max (Single-lobe) output power	60mW	< 10mW	1.4mW	104mW
Operation Mode	CW	Pulse	CW	CW

array has highly uniform single-mode performance. An excellent lasing phenomenon has been observed in our 6 × 6 array, and it exhibits a stable single-lobe/circular far-field pattern with a narrow FWHM divergence angle ($4° \sim 7°$) under the full range of bias current and a high maximum single-lobe output power (104 mW) under CW operation.

References

[1] F. Koyama, S. Kinoshita, and K. Iga, "Room-temperature continuous wave lasing characteristic of a GaAs vertical cavity surface-emitting laser," *Appl. Phys. Lett.*, vol. 55, no. 3, pp. 221–222, Jul. 1989.

[2] M. E. Warren, P. L. Gourley, G. R. Hadley, G. A. Vawter, T. M. Brennan, B. E. Hammons, and K. L. Lear, "On-axis far-field emission from two-dimensional phase-locked vertical cavity surface-emitting laser arrays with an integrated phase-corrector," *Appl. Phys. Lett.*, vol. 61, no. 13, pp. 1484–1486, Sep. 1992.

[3] M. Orenstein, E. Kapon, J. P. Harbison, L. T. Florez, and N. G. Stoffel, "Large two-dimensional arrays of phase-locked vertical cavity surface emitting lasers," *Appl. Phys. Lett.*, vol. 60, no. 13, pp. 1535–1537, Mar. 1992.

[4] A. Haglund, C. Carlsson, J. S. Gustavsson, J. Halonen, and A. Larsson, "A comparative study of the high-speed digital modulation performance of single- and multimode oxide confined VCSELs for free space optical interconnects," in *Proc. SPIE*, Jun. 2002, vol. 4649, pp. 272–280.

[5] P. Moser, J. A. Lott, P. Wolf, G. Larisch, A. Payusov, N. N. Ledentsov, and D. Bimberg, "Energy-efficient oxide-confined 850-nm VCSELs for long-distance multimode fiber optical interconnects," *IEEE J. Sel. Topics Quantum Electron.*, vol. 19, no. 2, p. 7 900 406, Mar./Apr. 2013.

[6] J.-W. Shi, J.-C. Yan, J.-M. Wun, J. Chen, and Y.-J. Yang, "Oxide-relief and Zn-diffusion 850 nm vertical-cavity surface-emitting lasers with extremely low energy-to-data-rate ratios for 40 Gbit/sec operations," *IEEE J. Sel. Topics Quantum Electron.*, vol. 19, no. 2, p. 7 900 208, Mar./Apr. 2013.

[7] R. Szweda, "VCSELs resurgent," *III-Vs Rev. Adv. Semicond. Mag.*, vol. 17, no. 8, pp. 28–31, Nov. 2004.

[8] J. A. Reagan, H. Liu, and J. F. McCalmont, "Laser diode based new generation lidars," in *Proc. IGARSS Symp.*, May 1996, pp. 1535–1537.

[9] J.-F. Seurin, G. Xu, B. Guo, A. Miglo, Q. Wang, P. Pradhan, J. D. Wynn, V. Khalfin, W.-X. Zou, C. Ghosh, and R. V. Leeuwen, "Efficient vertical-cavity surface-emitting lasers for infrared illumination applications," in *Proc. SPIE*, vol. 7952, *Vertical-Cavity Surface-Emitting Lasers XV*, Feb. 2011, p. 79520G.

[10] Å. Haglund, J. S. Gustavsson, J. Vukuši, P. Modh, and A. Larsson, "Single fundamental mode output power exceeding 6 mW from VCSELs with a shallow surface relief," *IEEE Photon. Technol. Lett.*, vol. 16, no. 2, pp. 368–370, Feb. 2004.

[11] J.-W. Shi, C.-C. Chen, Y.-S. Wu, S.-H. Guol, and Y.-J. Yang, "High-power and high-speed Zn-diffusion single fundamental mode vertical-cavity surface-emitting lasers at 850 nm wavelength," *IEEE Photon. Technol. Lett.*, vol. 20, no. 13, pp. 1121–1123, Jul. 2008.

[12] A. Furukawa, S. Sasaki, M. Hoshi, A. Matsuzono, K. Moritoh, and T. Baba, "High-power single-mode vertical-cavity surface-emitting lasers with triangular holey structure," *Appl. Phys. Lett.*, vol. 85, no. 22, pp. 5161–5163, Nov. 2004.

[13] D. F. Siriani and K. D. Choquette, "Electronically controlled two-dimensional steering of in-phase coherently coupled vertical-cavity laser arrays," *IEEE Photon. Technol. Lett.*, vol. 23, no. 3, pp. 167–169, Feb. 2011.

[14] D. Zhou and L. J. Mawst, "High-power single-mode antiresonant reflecting optical waveguide-type vertical-cavity surface-emitting lasers," *IEEE J. Quantum Electron.*, vol. 38, no. 12, pp. 1599–1606, Dec. 2002.

[15] L. Bao, N.-H. Kim, L. J. Mawst, N. N. Elkin, V. N. Troshchieva, D. V. Vysotsky, and A. P. Napartovich, "Near-diffraction-limited coherent emission from large aperture antiguided VCSEL arrays," *Appl. Phys. Lett.*, vol. 84, no. 3, pp. 320–322, Jan. 2004.

[16] E. W. Young, K. D. Choquette, S. L. Chuang, K. M. Geib, A. J. Fischer, and A. A. Allerman, "Single-transverse-mode vertical-cavity lasers under continuous and pulsed operation," *IEEE Photon. Technol. Lett.*, vol. 13, no. 9, pp. 927–929, Sep. 2001.

[17] J. Ko, E. R. Hegblom, Y. Akulova, N. M. Margalit, and L. A. Coldren, "AlInGaAs/AlGaAs strained-layer 850 nm vertical-cavity lasers with very low thresholds," *Electron. Lett.*, vol. 33, no. 18, pp. 1550–1551, Aug. 1997.

[18] N. Tansu, D. Zhou, and L. J. Mawst, "Low-temperature sensitive, compressively strained InGaAsP active $(\lambda = 0.78 - 0.85\ \mu\text{m})$ region diode lasers," *IEEE Photon. Technol. Lett.*, vol. 12, no. 6, pp. 603–605, Jun. 2000.

[19] S. B. Healy, E. P. O'Reilly, J. S. Gustavsson, P. Westbergh, A. Haglund, A. Larsson, and A. Joel, "Active region design for high-speed 850-nm VCSELs," *IEEE J. Quantum Electron.*, vol. 46, no. 4, pp. 506–512, Apr. 2010.

[20] J.-W. Shi, W.-C. Weng, F.-M. Kuo, Y.-J. Yang, S. Pinches, M. Geen, and A. Joel, "High-performance Zn-diffusion 850-nm vertical-cavity surface-emitting lasers with strained InAlGaAs multiple quantum wells," *IEEE Photon. J.*, vol. 2, no. 6, pp. 960–966, Dec. 2010.

[21] S. Noda, "Photonic crystal lasers-ultimate nanolasers and broad-area coherent lasers [Invited]," *J. Opt. Soc. Amer. B*, vol. 27, no. 11, pp. B1–B8, Nov. 2010.

[22] J.-W. Shi, Z.-R. Wei, K.-L. Chi, J.-W. Jiang, J.-M. Wun, I.-C. Lu, J. Chen, and Y.-J. Yang, "Single-mode, high-speed, and high-power vertical-cavity surface-emitting lasers at 850 nm for short to medium reach (2 km) optical interconnects," *IEEE/OSA J. Lightw. Technol.*, Dec. 2013, to be published.

[23] J.-W. Shi, J.-L. Yen, C.-H. Jiang, K.-M. Chen, T.-J. Hung, and Y.-J. Yang, "Vertical-cavity surface-emitting lasers (VCSELs) with high-power and single-spot far-field distributions at 850 nm wavelength by use of petal-shaped light-emitting apertures," *IEEE Photon. Technol. Lett.*, vol. 18, no. 3, pp. 481–483, Mar. 2006.

[24] P. B. Subrahmanyam, Y. Zhou, L. Chrostowski, and C. J. Chang-Hasnain, "VCSEL tolerance to optical feedback," *Electron. Lett.*, vol. 41, no. 21, pp. 1178–1179, Oct. 2005.

[25] K. Otsuka, K. Sakai, Y. Kurosaka, J. Kashiwagi, W. Kunishi, D. Ohnishi, and S. Noda, "High-power surface-emitting photonic crystal laser," in *Proc. IEEE LEOS/2007 Annu. Meet.*, Orlando, FL, USA, Oct. 2007, pp. 562–563.